Mechanistic Studies on ADAMTS13 Catalysis

Enrico Di Stasio,* Stefano Lancellotti,† Flora Peyvandi,§ Roberta Palla,§ Pier Mannuccio Mannucci,§ and Raimondo De Cristofaro†‡§

*Institute of Biochemistry and Clinical Biochemistry, †Department of Internal Medicine and Medical Specialties, and ‡Hemostasis Research Centre, Catholic University School of Medicine, Rome, Italy; and §A. Bianchi Bonomi Hemophilia and Thrombosis Center, University of Milan and Department of Medicine and Medical Specialties, Istituto di Ricovero e Cura a Carattere Scientifico Maggiore Hospital, Mangiagalli and Regina Elena Foundation, Luigi Villa Foundation, Milan, Italy

ABSTRACT The zinc-protease a disintegrin-like and metalloprotease with thrombospondin type I repeats (ADAMTS13) cleaves the Tyr^{1605}-Met^{1606} peptide bond of von Willebrand factor (VWF), avoiding the accumulation of ultra large VWF multimers. Hydrolysis by ADAMTS13 of a VWF analog (Asp^{1596}-Arg^{1668} peptide, fluorescence energy transfer substrate [FRETS]-VWF73) was investigated by a fluorescence quenching method (FRETS method) from 15°C to 45°C and pH values from 4.5 to 10.5. The catalysis was influenced by two ionizable groups, whose pK_a values were equal to 6.41 ± 0.08 (ionization enthalpy = 32.6 ± 1.7 kJ/mol) and 4 ± 0.1 (ionization enthalpy = 3.8 ± 0.4 kJ/mol), whereas these values were equal to 6 ± 0.1 and 4.1 ± 0.1, respectively, in Co^{2+}-substituted ADAMTS13. The catalytic process of FRETS-VWF73 hydrolysis showed negative activation entropy (−144 kJ/mol), suggesting that the transition state becomes more ordered than the ground state of the reactants. The k_{cat}/K_m values were not linearly correlated with temperature, as expression of change of the kinetic "stickiness" of the substrate. The Met^{1606}-Arg^{1668} peptide product acted as hyperbolic mixed-type inhibitor of FRETS-VWF73 hydrolysis. Asp^{1653}, Glu^{1655}, Glu^{1660}, Asp^{1663}, together with the hydrophilic side chain of Thr^{1656} were shown to form a "hot spot" in the VWF A2 sequence, which drives the molecular recognition and allosteric regulation of binding to ADAMTS13. The interaction of the Met^{1606}-Arg^{1668} region of VWF with ADAMTS13 involves basic residues of the protease and is thus progressively inhibited at pH values >8.50. A molecular model of the FRETS-VWF73 showed that the substrate can fit into the active site only if ADAMTS13 assumes a C-like shape and, interacting with the acidic 1653–1668 region of VWF, properly orients the Tyr^{1605}-Met^{1606} peptide bond for the cleavage by the zinc-aquo complex in the active site.

INTRODUCTION

A disintegrin-like and metalloprotease with thrombospondin type I repeats (ADAMTS13) is a member of the ADAMTS family of metalloproteases (1) constituted by a multidomain enzyme that cleaves von Willebrand factor (VWF) at the peptide bond between Tyr^{1605} and Met^{1606}, located in the VWF A2 domain. On cleavage, one N-terminal and one C-terminal fragment are generated from the VWF monomer (2–5). Pathological perturbations of the ADAMTS13/VWF proteolytic interaction are responsible for either thrombotic microangiopathies or hemorrhagic syndromes in type 2A von Willebrand diseases (6–11). Modulation of the ADAMTS13/VWF interaction is critical for an efficient proteolysis and involves both VWF and ADAMTS13. The latter binds to VWF under static conditions and under conditions of venous (2.5 dyn/cm^2) and arterial (30 dyn/cm^2) shear stress. This interaction, however, is unproductive for proteolysis unless shear stress is high enough to stretch VWF and expose the buried A2 domain for cleavage (12–15). Under static conditions, ADAMTS13 cleaves VWF only under denaturing conditions (8), whereas under conditions of high shear stress found in the microvasculature VWF proteolysis is extremely rapid and occurs without denaturing agents (3,16,17). Fluid shear stress alters the conformation of VWF so that the binding and catalysis of ADAMTS13 takes place at the VWF A2 domain (13). The Tyr^{1605}-Met^{1606} peptide bond is in fact buried within the VWF A2 domain under static conditions and cannot be recognized by ADAMTS13 (12,14,15). Recent studies have also shown that the binding of the platelet receptor of VWF, i.e., the Glycoprotein Ib (GpIbα), is able to induce conformational changes in the A1–A2 domains of VWF, responsible for an enhanced rate of cleavage by the metalloprotease (18,19). On the contrary, binding of chloride ions to the A1 domain of VWF inhibits proteolysis by ADAMTS13, inducing conformational transitions in the A1–A2 VWF domains, which make the cleavable peptide bond in the A2 domain unavailable to proteolysis (8,20,21). Thus, only in the presence of specific biophysical or biochemical factors, VWF molecules assume a proper conformational state available to proteolytic attack by ADAMTS13. Knowledge of the factors that can modulate this interaction is particularly relevant, as it may help to unravel the mechanisms through which the reaction is inhibited in several clinical settings. Among biochemical factors, protons play a relevant role in modulating the activity of metalloproteases and pH may change in vivo, having different values inside and outside the cellular compartment. Previous data showed that the velocity of ADAMTS13 hydrolysis of a synthetic

Submitted February 16, 2008, and accepted for publication May 9, 2008.

Address reprint requests to R. De Cristofaro, Haemostasis Research Center, Department of Internal Medicine, Catholic University School of Medicine, Largo F. Vito 1, 00168 Rome, Italy. Tel.: 30-06-30154438; Fax: 39-06-30155915; E-mail: rdecristofaro@rm.unicatt.it.

Editor: David W. Piston.

0006-3495/08/09/2450/12 $2.00

doi: 10.1529/biophysj.108.131532

peptide shows a maximum under acidic conditions, although no systematic study of the pH-dependence of steady state kinetic parameters was carried out (22). This pH-dependent activity of ADAMTS13 seems rather unusual if compared to other zinc-proteases, and especially matrix metalloproteases and ADAMS (23,24), which show maximum activity at pH values >7. The scenario of the pH-dependence of the activity of ADAMTS13 is complicated further by previous findings showing that under mild denaturing conditions ADAMTS13 cleaves natural VWF multimers at a pH optimum >8 (8). Unfortunately, both the need to use denaturing agents under static conditions to investigate the ADAMTS13/VWF interaction and the multimeric nature of the substrate renders practically impossible the study of the pH- and temperature-dependence of the catalytic parameters of cleavage of native VWF multimers. The discovery of a fluorescent peptide substrate spanning from Asp^{1596} to Arg^{1668} of the A2 domain of VWF (fluorescence energy transfer substrate [FRETS]-VWF73) (22) makes feasible a systematic study of the steady-state kinetic parameters for its hydrolysis as a function of pH and temperature, that is still elusive. The use of this fluorescent substrate and the Fluorescence quenching method (FRETS method) was applied to both native Zn^{2+}-ADAMTS13 and artificially Co^{2+}- and Ni^{2+}-substituted ADAMTS13 to investigate the effects of pH and temperature on the protease activity of the enzyme. Finally, the use of different peptides synthesized from the Asp^{1596}-Arg^{1668} substrate sequence allowed us to investigate whether the interaction with ADAMTS13 is allosterically regulated by interactions with different regions of the substrate and whether protons play a role in such a regulation. The aspect concerning the pH-dependent modulation of ADAMTS13/VWF interaction is physiologically relevant because after extrusion from intracellular granules, VWF indeed may experience large variations in environmental conditions, as pH and ionic strength. These mechanistic studies allowed us to obtain initial informations on the recognition and cleavage mechanisms operating on the proteolytic processing of VWF by ADAMTS13.

MATERIALS AND METHODS

Purification of recombinant and plasma-derived human ADAMTS13

ADAMTS13 used in this study was either a recombinant His-tagged form, produced in HEK-293 cell line based on the reported gene sequence of the enzyme (25) and purified as previously described (20) or derived from human plasma (provided by the Transfusion Center of the Catholic University School of Medicine of Rome from outdated units of fresh frozen plasma). The latter preparation was used for experiments dealing with exchange of the catalytic zinc with cobalt ion. For this preparation the original step of the purification procedure, i.e., ammonium sulfate precipitation (20), was replaced by an affinity chromatography using an anti-ADAMTS13 polyclonal antibody. Briefly, 1 mg of rabbit anti-human ADAMTS13 polyclonal antibody, raised against amino acids 1128–1427 of the enzyme, was purchased from Santa Cruz Biotechnology (Santa Cruz, CA). The purified IgGs were immobilized through the carbohydrate moiety of the Fc region to 2 mL of Affi-Gel Hz Activated Support from Bio-Rad Laboratories (Hercules, CA) according to the manufacturer's procedure. One mM (final concentration) phenyl-methyl-sulfonyl-fluoride (PMSF) was added to 1 L of outdated fresh frozen plasma, which was percolated at 4°C overnight on the Affi-Gel Hz resin coupled to anti-ADAMTS13 polyclonal antibody, at a flow rate of 1.5 mL/min. After the entire amount of plasma was percolated, the column was washed with 10 mM Hepes, 0.15 M NaCl, pH 7.40 until the absorbance at 280 nm was zeroed. The bound protein was eluted by 0.1 M glycine buffer, pH 3. A small amount (≈200 μL) of 1 M Tris-HCl buffer pH 8.5 was previously added to the collecting test tubes to neutralize the pH of the glycine buffer and obtain a final pH value of ~7. The pooled material contained a major component of ~180 kDa and minor additional bands, that were eliminated following the previously described chromatographic procedures (20). The final material was tested by SDS-PAGE using a 4%–12% acrylamide gradient under reducing conditions, which showed a single band with a molecular mass of ~180 kDa. The concentration of the purified enzyme was determined using an E(280 nm) (mg/mL, 1 cm) = 1.45, calculated using the method of Pace et al. (26). The purified enzyme was aliquoted and stored at −80°C in stock solutions at ~0.3 mg/mL containing 10 mM Hepes, 0.15 M NaCl, 5 mM $CaCl_2$, pH 7.5.

Preparation of Co^{2+}-substituted ADAMTS13

Apo-ADAMTS13 was prepared by treating a solution of 100 μg of ADAMTS13 in 10 mM sodium acetate, pH 5.5, with 5 mM-I,10-phenanthroline for 1 h at 4°C (final volume, 1 mL). The enzyme solution was then dialyzed against 2 L of 10 μM of 1,10-phenanthroline for 2 h, and then against 4 L of 1 mM $CoCl_2$ (99.999% pure; Sigma-Aldrich, Milano, Italy) overnight. This $CoCl_2$ solution and all subsequent buffers were made in glass-distilled deionized water that had been additionally treated with Chelex100 (Bio-Rad). The efficiency of incorporation of Co^{2+} into apo-ADAMTS13 was checked by measuring the ratio between the concentration of ADAMTS13, determined both spectrophotometrically (at 280 nm) and by a commercial ELISA assay (Imubind ADAMTS13 antigen, American Diagnostica, Instrumentation Laboratory, Milan, Italy), and its protease activity measured by FRETS-VWF73. The concentrations of Co^{2+}- and Zn^{2+}-ADAMTS13 measured spectrophotometrically and by ELISA were in good agreement (difference within 8% deviance). After the extraction of Zn^{2+} ions from ADAMTS13 and elimination of phenanthrolene by extensive dialysis, the activity of the enzyme toward FRETS-VWF73 was completely absent. The lack of any artificial inactivation of ADAMTS13 by the process of extracting zinc was checked by re-incorporating zinc ions by extensive dialysis into the catalytic site of the apo-enzyme and measuring its catalytic properties in comparison with the untreated enzyme. Co^{2+}-ADAMTS13 preparation was kept in buffer solutions containing a final concentration of 100 μM $CoCl_2$ and 5 mM $CaCl_2$. Before any functional assay, Co^{2+}-ADAMTS13 solutions were freed from Co^{2+} ion by gel filtration on DG-10 columns (Bio-Rad) equilibrated with appropriate buffer solution without cobalt chloride.

Determination of kinetic parameters of FRETS-VWF cleavage by FRETS method

The substrate used for the enzymatic assays was DRE-A2pr(Nma)-APNL-VYMVTG-A2pr(Dnp)-PASDEIKRLPGDIQVVPIGVGPNANVQELER-IGWPNAPILIQDFETLPREAPDLVLQR, corresponding to the region from D1596 to R1668 of VWF. Called FRETS-VWF73, the substrate was synthesized by Thermo Electron Corporation GmbH (Ulm, Germany). When ADAMTS13 cleaves the bond between Y10 and M11 in FRETS-VWF73, the fluorescence at λ_{em} between 420 and 460 nm and $\lambda_{ex} = 340$ nm increases in proportion to the release of Nma fluorophore from the internal Dnp quencher (see Fig. S1 in Supplementary Material, Data S1). Other shorter not fluorescent peptides, that are Met^{1606}-Phe^{1654}, Met^{1606}-Leu^{1657}, Met^{1606}-Ala^{1661}, Met^{1606}-Leu^{1664}, and Met^{1606}-Arg^{1668} were synthesized by PRIMM

s.r.l. (Milano, Italy). The fluorescent substrate was dissolved in 50% dimethylsulfoxide at a concentration of 5 mM. In the functional assays, the final concentration was always ≤0.05% (w/v), that did not affect the protease activity. The hydrolyzed peptide was monitored by exciting the substrate at 340 nm and measuring the fluorescence at 450 nm (bandwidth of 5 nm at both excitation and emission wavelength). Assays were carried out in 5 mM Na-acetate, 5 mM Bis-Tris, 5 mM Tris, 10 mM CHES, 150 mM NaCl, 25 mM $CaCl_2$, over the pH range spanning from 4.5 to 10.5. This four buffer system allowed to keep nearly constant the ionic strength of the solution over the entire pH range. The Michaelis constants of FRETS-VWF73 hydrolysis were calculated using 0.5–2.5 nM purified human ADAMTS13 and 1–20 μM FRETS-VWF73. The initial velocity of FRETS-VWF73 hydrolysis by ADAMTS13 was computed by a linear regression of the initial 20–40 points ($r > 0.97$) and always when not more than 5% (1 μM) of the substrate was hydrolyzed, according to the principles of steady-state enzyme kinetics (27). Thus, the reference curve for the conversion of the fluorescence signal into concentration of cleaved substrate was carried out constructing a reference curve (8 dilutions, dilution factor = 1.5) with a solution of FRETS-VWF73 at known concentration (1 μM) exhaustively hydrolyzed for 24 h by 0.5 nM ADAMTS13. Furthermore, the emission spectrum of the hydrolyzed FRETS-VWF73 was analyzed between 400 and 500 nm at pH values spanning from 4.5 to 10.50, and at different temperatures ranging from 15°C to 45°C, to assess any influence of these parameters on the fluorescence properties of the product. The kinetic parameters, k_{cat} and K_m, were determined as the mean of at least two independent measurements. The interassay CV was ~8%.

Fluorescence emission spectra at 450 nm ($\lambda_{ex} = 340$ nm) were recorded in a 1-cm quartz cell, using an Eclipse spectrofluorometer (Varian, Leini, Italy), equipped with a thermostated cell holder connected to a Varian Cary Peltier temperature controller.

Kinetic mechanism of ADAMTS13 activity studied as a function of temperature

The proteolytic cycle of ADAMTS13 should follow Scheme 1:

$$E + S \underset{k_{-1}}{\overset{k_1}{\rightleftarrows}} ES \xrightarrow{k_2} E + P1 + P2, \qquad \text{(Scheme 1)}$$

where E and ES are the free and Michaelis forms of ADAMTS13, whereas P_1 and P_2 are the tyrosine-containing and methionine-containing released peptide products, respectively. According to the classical Michaelis-Menten scheme we have (27):

$$k_{cat} = k_2 \quad (1)$$

$$K_m = (k_{-1} + k_2)/k_1 \quad (2)$$

hence:

$$k_{cat}/K_m = k_1 k_2/(k_{-1} + k_2). \quad (3)$$

The k_2/k_{-1} ratio is the ''stickiness'' of the substrate, that expresses the tendency of the substrate to dissociate more slowly from its complex formed with the enzyme than it reacts to yield products, i.e., $k_2 > k_{-1}$. The temperature-dependence of the rate constants contained in Eqs. 1 and 3 was studied using the Arrhenius relations (28):

$$k_{cat} = k_2^{\circ}\exp[-(E_2/R)(1/T - 1/T_0)] \quad (4)$$

where k_1° and k_2° are the values of k_1 and k_2 at the reference temperature, E_1 and E_2 are the activation energies associated with k_1 and k_2 and R is the gas constant (8.314 J/K mol). From the simultaneous analysis of the temperature dependence of k_{cat}/K_m and k_{cat} parameters the values of k_1, k_{-1}, and k_2 can be obtained together with the corresponding activation energies. Because T_0 can be set to any value, the parameters can be calculated over the entire temperature range studied.

Further analysis according to the Eyring's transition state theory led to calculation of the values of the activation enthalpy and entropy pertaining to the formation of the transition state leading to cleavage of the FRETS-VWF73 substrate. Accordingly:

$$\ln(k_{cat}/T) = (-\Delta H^{\ddagger}/R)(1/T) + \ln k_B/h + \Delta S^{\ddagger}/R, \quad (6)$$

where k_B = Boltzmann's constant = $1.381 \times 10^{-23}\, J\, K^{-1}$, h is the Planck's constant (6.626×10^{-34} J sec), $\Delta H^{\ddagger}$ = activation enthalpy ($kJ \times mol^{-1}$) and $\Delta S^{\ddagger}$ = activation entropy ($J \times mol^{-1} \times K^{-1}$). Hence the free energy was calculated using the relation (29):

$$\Delta G^{\ddagger} = \Delta H^{\ddagger} - T\Delta S^{\ddagger}. \quad (7)$$

In our experiments only steady-state initial velocities of FRETS-VWF73 hydrolysis (hydrolyzed peptide <10% total substrate) were analyzed to avoid the problem of inhibition of the ADAMTS13 activity by high concentrations of released P_2 (see below). The FRETS-VWF73 concentrations used in the temperature experiments were between 0.3 and 20 μM, that allowed in all cases to compute the Michaelis parameters, avoiding the phenomenon of the inner filter effect (30), which was evident at concentrations >20 μM. Control experiments were carried out to measure the temperature-dependence of the emission spectrum of the cleaved FRETS-VWF73. The temperature-dependence of the Michaelis parameters was studied from 15°C to 45°C in the four-buffer system described above at pH 6.00, where the maximum activity was observed.

Effect of pH on FRETS-VWF73/ADAMTS13 interaction

The effect of pH on FRETS-VWF73 hydrolysis by ADAMTS13 was investigated using substrate concentration <K_m of the reaction. Under this condition, the kinetics of substrate hydrolysis was followed at selected time intervals to compute the pseudo-first order rate constant of the reaction, k^{obs}, that was equal to the relation $k^{obs} = (k_{cat}/K_m)e^{\circ}$ (27), where e° is the total concentration of ADAMTS13. The fluorescence signals were thus transformed in product concentration observed at each time point, P_t, as indicated above. These values were fitted to the equation $P_t = P_{max}(1 - \exp[-k^{obs} \times t])$, where P_{max} is the maximum concentration of released product at time = ∞.

The effect of pH on the observed k_{cat}/K_m values of FRETS-VWF73 hydrolysis was analyzed, assuming the existence of two ionizable groups involved in catalysis. Accordingly (27):

$$k_{cat}/K_m^{obs} = [(k^1 \times P_1)/(1 + P_1)] - [(k^1 - k^2) \times P_2/(1 + P_2], \quad (8)$$

where k^1 is the maximum value of k_{cat}/K_m corresponding to the middle pH form, k^2 is the value of k_{cat}/K_m corresponding to the high pH form, P_1 = alog(pH − pK_{a1}) and P_2 = alog(pH − pK_{a2}) and pK_{a1} and pK_{a2} are the acidic and basic pK_a values controlling the catalytic activity of ADAMTS13. In this analysis, it was assumed that low pH species has no activity. This assumption was based on the known function of His residues that chelate the catalytic

$$k_{cat}/K_m = \frac{k_1^{\circ}k_2^{\circ}\exp[-((E_1 + E_2)/R)(1/T - 1/T_0)]}{\{k_{-1}^{\circ}\exp[-(E_1/R)(1/T - 1/T_0)] + k_2^{\circ}\exp[-(E_2/R)(1/T - 1/T_0)]\}}, \quad (5)$$

Zn^{2+}. In fact, at pH <5 the protonation of the His imidazole side chain affects the interaction with Zn^{2+}, blocking the catalytic cycle

The values of k_{cat}/K_m were then analyzed as a function of pH at six different temperatures ranging from 15°C to 37°C by a nonlinear least-square fitting procedure. The pK_a values of the ionizable groups derived from the fitting procedure were analyzed by the Van t' Hoff relation (31) to calculate the values of the ionization enthalpy of the groups involved in the catalytic process. All analyses were carried out using the software Grafit (Erithacus, Horley Surrey, UK).

Experimentally, the pH-dependent changes of k_{cat}/K_m values were studied using a micromethod using 200 μl of total solution containing 0.5 nM ADAMTS13 and 1–2 μM of the FRETS-VWF73 substrate in the four-buffer system described above, analyzing 25 different pH values, ranging from 4.50 to 10.50. The stability of the purified ADAMTS13 over the pH range studied was confirmed previously through incubation of the enzyme for 180 min in buffer at a given pH. The initial velocity of hydrolysis of 1 μM FRETS-VWF73 by ADAMTS13 without previous incubation and after 180 min incubation in the four buffer system at pH spanning from 4.50 to 10.5 showed that only at extreme pH values (4.50 and 10.5).the activity of the incubated enzyme was ≈7% lower than that observed in not incubated ADAMTS13. Based on the limited loss of activity, no systematic correction was applied to the kinetic data. All the enzymatic assays were followed in a Varian Eclipse spectrofluorometer, equipped with a microplate reader, using 96-well polystyrene microplates (Corning nonbinding surface). This experimental strategy allowed us to follow simultaneously the course of the substrate's hydrolysis under different pH values, thus minimizing the error arising from interassay variability.

Effect of the Met^{1606}-Arg^{1668} peptide on the hydrolysis of the FRETS-VWF73 by ADAMTS13

Recent findings showed that the C-terminal region of the VWF-73 peptide spanning from Glu^{1660} to Arg^{1668} is engaged in interaction with the spacer domain of ADAMTS13 and inhibits the hydrolysis of the VWF-73 peptide (32,33). This effect was investigated in this study as a function of pH, using purified different synthetic peptides contained in the VWF-73 substrate, such as Met^{1606}-Phe^{1654}, Met^{1606}-Leu^{1657}, Met^{1606}-Ala^{1661}, Met^{1606}-Leu^{1664}, and Met^{1606}-Arg^{1668}. Based on the experimental findings (see Results), the effect of the Met^{1606}-Arg^{1668} peptide on FRETS-VWF73 was best analyzed using an expanded form of Scheme 1, as follows:

$$\begin{array}{ccccc} E + S & \underset{k_{-1}}{\overset{K_s}{\rightleftharpoons}} & ES & \xrightarrow{k_2} & E + P1 + P2 + I \\ Ki\updownarrow & & \alpha Ki\updownarrow & & \\ EI + S & \overset{\alpha K_s}{\rightleftharpoons} & EIS & \xrightarrow{\beta k_2} & EI + P1 + P2 \end{array} \quad \text{(Scheme 2)}$$

where α and β are the factors by which K_i and k_2 change, respectively, when the ternary complex E·I·S is formed, and K_s is the dissociation binding constant of the substrate. Notably, for the principle of thermodynamic balance we obtain that $K_s \times \alpha K_i = K_i \times \alpha K_s$. Thus, when K_m of FRETS-VWF73 hydrolysis approaches K_s (for instance at $T \geq 25$°C), the former parameter changes as a function of I concentration by the same factor α, as K_i does as a function of FRETS-VWF73 concentration. This effect was verified in our experimental set up at pH 7.50 and 25°C. Thus, the initial velocities of VWF-73 hydrolysis by ADAMTS13 were fitted to the following equation, according to a classical scheme of hyperbolic mixed-type inhibition (34):

$$v_i = k_{cat} E S Z^0 / [(K_m Z^1) + (S Z^2)], \quad (9)$$

where

$$Z^0 = 1 + (\beta I/\alpha K_i)$$
$$Z^1 = 1 + (I/K_i)$$
$$Z^2 = 1 + (I/\alpha K_i).$$

Hydrolysis of FRETS-VWF73 was analyzed by RP-HPLC. Briefly, at the end of incubation, stopped by 100 mM EDTA, the solutions was chromatographed on a C18 RP-HPLC column (RP-318 column, 5-μm pore size; Bio-Rad, Milano, Italy), using the following conditions: 10% $CHCN_3$ in 0.1% TFA for 5 min, 10%–50% $CHCN_3$ in 0.1% TFA for 45 min. The eluted peptides were detected simultaneously both by a UV/VIS spectrophotometric device at 210 nm (model 2075, Jasco, Easton, MD) and spectrofluorometric detector (FP-2020, Jasco) using a $\lambda_{exc} = 280$ nm and a $\lambda_{em} = 340$ nm. The initial velocities were taken by a linear regression of the five concentrations of FRETS-VWF73 measured as a function of time (with $r > 0.92$), when <5% substrate was hydrolyzed by ADAMTS13. This experimental procedure was adopted to avoid product inhibition phenomena. The reference curve for the conversion of the spectrofluorometric signals into concentration of cleaved substrate was carried out as described previously for the FRETS method. The effect of Met^{1606}-Arg^{1668}, over a concentration range from 0.5 to 16 μM, was studied at pH 6.0, 7.50, and 9.50 at 25°C, whereas the other peptides were studied at only pH 7.50 using a maximal concentration of 20 μM.

Modeling of FRETS-VWF73 and spacer domain of ADAMTS13

The FRETS-VWF73 peptide was modeled using its primary sequence homology to the VWF A3 domain and the coordinates for the crystal structure of this domain (Protein Data Bank, code 1atz), according to the method detailed previously (14). The model of the final three-dimensional structure was built using the modeling package MODELLER, which satisfied the spatial restraints (36). The prediction of the secondary structure of the spacer domain of ADAMTS13 was produced using its primary sequence from Ser^{556} to Ala^{685} and the PsiPred and DisoPred programs (36–38).

RESULTS

Temperature studies

The fluorescence signal was inversely correlated to temperature, decreasing by ~0.6 fluorescence units/1°C under the experimental conditions of the study (see Figs. S1 and S2 in Data S1). Based on this finding, the reference curve to calculate the concentration of the product from the raw fluorescence data was constructed at each temperature. In our system, at 25°C and pH 6.0 the values of k_{cat} and K_m of FRETS-VWF73 hydrolysis by ADAMTS13 were 2.54 ± 0.03 sec^{-1}, and 4.6 ± 0.2 μM, respectively, in good agreement with previous findings (32,33,39). The k_{cat} values were linearly correlated to temperature, as expected for a simple A → B reaction following the Arrhenius law. Thus, the k_{cat} value reflects the k_2 rate constant of Scheme 1. By contrast, this was not the case for the K_m values, and consequently for k_{cat}/K_m as well, as shown in Fig. 1. Simultaneous fitting to Arrhenius equations (Eqs. 4 and 5) of experimental values of both k_{cat} and k_{cat}/K_m of FRETS-VWF73 hydrolysis allowed the computation of the kinetic rate constants and the relative activation energies, listed in Table 1. It is conspicuous that $E_{-1} > E_2$, indicating that the activation energy of FRETS-VWF73 dissociation from ADAMTS13 is higher than that needed for its hydrolysis. The ''stickiness'' of FRETS-VWF73 (k_2/k_{-1}) changed as a function of temperature, showing values listed in Table 1. At temperatures <25°C

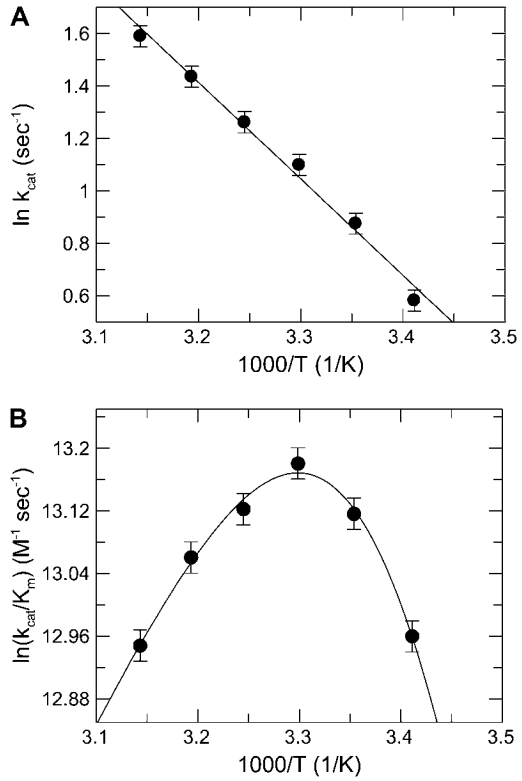

FIGURE 1 Arrhenius plot of k_{cat} (*A*) and k_{cat}/K_m (*B*) values of FRETS-VWF73 hydrolysis by ADAMTS13. The continuous lines were drawn according to Eqs. 4 and 5, with the best-fit parameter values listed in Table 1. In all the data sets the vertical bars represent the SD from two different determinations.

FRETS-VWF73 acts a sticky substrate, being the rate constant for its breakdown comparable or even higher than that for its dissociation from the active site of the enzyme. This is not the case at 37°C, as can be inferred from results reported in Table 1. At this temperature, in fact, the k_2/k_{-1} ratio was $\approx$0.1 and, in virtue of Eq. 3, the value of k_{cat}/K_m is about 10-fold lower than that of k_1. Moreover, being $k_{-1} > k_2$ at $T \geq 25$°C, in virtue of Eq. 2, K_m approaches progressively the value of K_d, that is the real equilibrium dissociation constant of FRETS-VWF73 binding to ADAMTS13. Over the temperature range from 15°C to 45°C, the Eyring's plot for the reactions of FRETS-VWF73 with ADAMTS13 shown in Fig. 2, allowed us to calculate the relevant activation thermodynamic parameters pertaining to the kinetic scheme of FRETS-VWF73 cleavage. The values of these parameters were: $\Delta H^{\ddagger} = 28 \pm 1.1$ kJ/mol, $\Delta^{S\ddagger} = -144 \pm 3.1$ kJ/mol K. At 25°C, $\Delta G^{\ddagger} = 70.9 \pm 4$ kJ/mol.

TABLE 1 Kinetic and thermodynamic parameters for the reaction of ADAMTS13 with FRETS-WF73

T (°C)	k_1 (M^{-1} sec^{-1})	k_{-1} (sec^{-1})	k_2 (sec^{-1})	k_2/k_{-1}
15	$4.40 \pm 0.2 \times 10^5$	0.61 ± 0.2	1.50 ± 0.06	2.45
20	$7.90 \pm 1.3 \times 10^5$	1.64 ± 0.6	1.89 ± 0.06	1.15
25	$1.39 \pm 0.4 \times 10^6$	4.10 ± 1.9	2.30 ± 0.05	0.56
30	$2.39 \pm 0.6 \times 10^6$	10.00 ± 5.7	2.86 ± 0.05	0.29
35	$3.96 \pm 29 \times 10^6$	23.70 ± 13	3.48 ± 0.06	0.15
40	$6.70 \pm 4 \times 10^6$	56.20 ± 38	4.21 ± 0.1	0.074
45	$7.31 \pm 5 \times 10^6$	70.50 ± 42	5.10 ± 0.16	0.073

The activation free energy of k_{+1} (E_1), k_{-1} (E_{-1}), and k_2 (E_2) was equal to 81.5 ± 20 kJ/mol, 135 ± 16 kJ/mol, and 30.5 ± 1.6 kJ/mol, respectively.

Effect of pH on k_{cat}/K_m of FRETS-VWF73 hydrolysis by ADAMTS13

Control experiments showed that the fluorescence signals were not appreciably affected by pH ranging from 4.5 to 10.5. Under the pseudo-first conditions of this study, the time course of FRETS-VWF73 cleavage allowed to reliably calculate the k_{cat}/K_m value of the reaction, as shown in Fig. 3. Analysis of the pH-dependence of k_{cat}/K_m values at each temperature (Eq. 8) over the pH range from 4.5 to 10.5 showed that two ionizable groups in the free form of the enzyme are involved in the catalytic cleavage of the FRETS-VWF73 peptide, as shown in Fig. 4 *a*. For Zn^{2+}-ADAMTS13, the calculated pK_{a1} value of 6.41 ± 0.08 at 25°C is compatible with a histidine group. The pK_a value of this group could be theoretically assigned even to a group of unliganded FRETS-VWF73. However, the absence of a histidine residue in the sequence of the substrate allowed to rule out such an involvement. We know that three His residues are present in the catalytic site of ADAMTS13 in the sequence His^{224}Glu-Ile-Gly-His^{228}-Ser-Phe-Gly-Leu-His^{234}, where His^{224}, His^{228}, and His^{234} should be engaged in the coordination of the zinc ion. The latter should be coordinated by a fourth ligand, which is hypothesized to be a water molecule bound to a zinc ion. The Van t' Hoff analysis of the pK_{a1} values showed that the standard enthalpy of its ionization was equal to 32.5 ± 1.8 kJ/mol, as shown in Fig. 4 *b*. The results of these temperature studies are consistent with the assignment of the

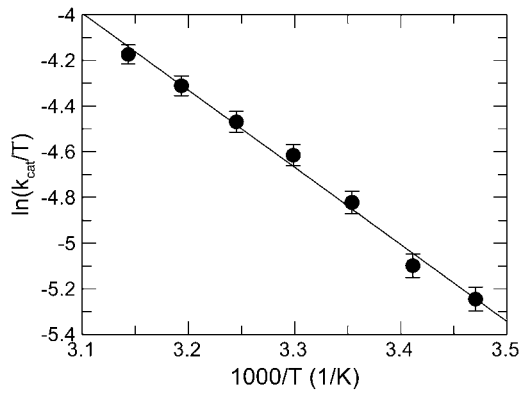

FIGURE 2 Eyring plot of k_{cat} values of FRETS-VWF73 hydrolysis by ADAMTS13. The slope ($r = -0.996$) and the intercept allowed to calculate the relevant activation thermodynamic parameters: $\Delta H^{\ddagger} = 28 \pm 1.1$ kJ/mol, $\Delta S^{\ddagger} = -144 \pm 3.1$ J/mol K. At the standard temperature of 25°C, $\Delta G^{\ddagger} = 70.9 \pm 4$ kJ/mol.

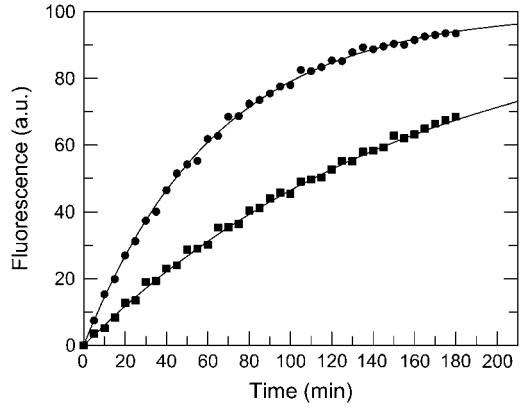

FIGURE 3 Examples of the kinetics of FRETS-VWF73 cleavage (1 μM) by 0.5 nM ADAMTS13 in the four-buffer system solution at pH 5.0 (■) and 10.0 (●) and T = 25°C. For sake of clarity, the fluorescence signal at time = ∞ was set at 100% and corresponded to 1 μM cleaved FRETS-VWF73. The continuous lines were drawn according to a simple first order kinetics with the best-fit k_{cat}/K_m values equal to 5.2 ± 0.1 × 10^5 M^{-1} sec^{-1} and 2.03 ± 0.06 × 10^5 M^{-1} sec^{-1} for pH 5 and 10, respectively.

general acid either to a H-N_2(His) atom or a metal-bound water molecule (40). To overcome this uncertainty, we measured the pK_a of the ionizable group involved in the catalytic mechanisms of the Co^{2+}-substituted ADAMTS13. The process of Zn^{2+} extraction from the native enzyme did not alter its functional properties, as the reconstitution of the Zn^{2+}-ADAMTS13 from apo-ADAMTS13 was reversible and generated again an enzyme with values of k_{cat} and K_m of FRETS-VWF73 hydrolysis very close to those of the native form (k_{cat} of 2.1 ± 0.3 vs. 2.4 ± 0.2 sec^{-1}, and K_m of 4.5 ± 0.5 μM vs. 4.8 ± 0.4 μM, respectively). Co^{2+}-ADAMTS13 showed at pH 6.00 a reduced k_{cat}/K_m compared to that of the Zn^{2+}-ADAMTS13. This effect was caused by a minimal change of K_m (5.1 vs. 4.8 μM) and a significant decrease of k_{cat} value (1 vs. 2.4 sec^{-1}). It is noteworthy that substitution of zinc with nickel ion caused a much more marked decrease of the peptidase activity of ADAMTS13, which was almost inactive in the FRET assay. The replacement of metal ions in the active site of ADAMTS13 in studies concerning the pH-dependent amidase activity provided useful elements to try unraveling of the assignment of this ionizable group involved in the catalytic machinery. Theoretical and experimental studies showed that a metal ion-dependent shift in pK_a for metalloproteases reflects the ionization of the metal-coordinated water molecule bound to enzyme (41). On the contrary, the same pK_a value for different metal-substituted metalloproteases was shown to be due to a critical amino acid at the active site of the protease involved and not to an enzyme-metal-water complex (42). As shown in Fig. 4 *a*, the analysis of the k_{cat}/K_m values of FRETS-VWF73 hydrolysis by Co^{2+}-ADAMTS13 as a function of pH showed a significant change of the pK_a value of the Co^{2+}-substituted enzyme from 6.41 ± 0.08 in the Zn^{2+}-ADAMTS13 to 6 ± 0.09 in the Co^{2+}-substituted enzyme.

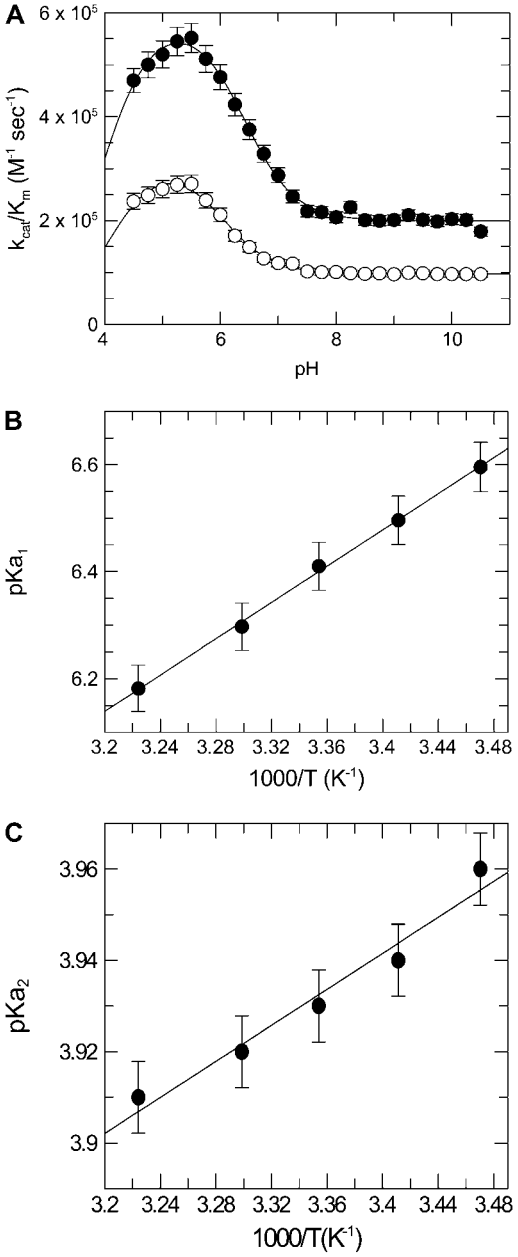

FIGURE 4 (*A*) Effect of pH on k_{cat}/K_m values of FRETS-VWF73 hydrolysis by both Zn^{2+}-ADAMTS13 (●) and Co^{2+}-ADAMTS13 (○) at 25°C. The continuous lines were drawn according to Eq. 8, with the best-fit pK_a values of 6.41 ± 0.08 and 4 ± 0.1 for Zn^{2+}-ADAMTS13 (k^1 = 5.9 ± 0.09 × 10^5 M^{-1} sec^{-1}, k^2 = 1.99 ± 0.03 × 10^5 M^{-1} sec^{-1}) and 6.01 ± 0.09 and 4.1 ± 0.13 (k^1 = 3.2 ± 0.08 × 10^5 M^{-1} sec^{-1} and k^2 = 0.98 ± 0.02 × 10^5 M^{-1} sec^{-1}) for Co^{2+}-ADAMTS13. (*B*) Van t' Hoff plot of the pK_{a1} of the ionizable group involved in the catalytic cycle of ADAMTS13. The straight line was drawn with the best-fit ΔH value equal to 32.5 ± 1.8 kJ/mol. (*C*) Van t' Hoff plot of the pK_{a2} of the ionizable group involved in the catalytic cycle of ADAMTS13. The straight line was drawn with the best-fit ΔH value equal to 3.8 ± 0.4 kJ/mol.

Thus, both the value of the standard ionization enthalpy equal to 28 kJ/mol, which is typical of water molecules (43), and the intrinsic pK_a value provided functional evidence that the pK_a value of 6.41 of Zn^{2+}-ADAMTS13 derives

from the metal-bound water molecule at the active site of the enzyme.

The second ionizable group involved in ADAMTS13 catalysis exhibited a lower pK_a value, equal to ~4 for both Zn^{2+}- and Co^{2+}-ADAMTS13 (Fig. 4 *a*). The standard enthalpy of ionization was equal to 3.8 ± 0.4, as shown by a van't Hoff plot in Fig. 4 *c*. This value is typical for ionization of a carboxylate group (44). Due to the presence of a glutamate at position 225 of ADAMTS13, in the region engaged in the coordination of the catalytic zinc ion, we could reasonably assign to Glu225 the pK_{a2} value measured in these experiments.

Inhibition of ADAMTS13 by the Met^{1606}-Arg^{1668} peptide

Extensive analysis of the experimental data set pertaining to the inhibitory effect of Met^{1606}-Arg^{1668} peptide on FRETS-VWF73 hydrolysis by ADAMTS13 showed that this phenomenon was best described by a hyperbolic mixed-type mechanism. Two other models were analyzed: 1) a pure noncompetitive inhibition, and 2) a linear mixed-type inhibition (45). The minimization procedure provided in fact a reduced χ^2 equal to 4.454×10^{-4} for the hyperbolic mixed-type, $1.6 - 10^{-3}$ for the linear mixed-type, and 4.86×10^{-3} for the noncompetitive inhibition model. *F*-testing of the results obtained at pH 6.0 with the hyperbolic and linear mixed-type inhibition model gave a probability value $= 3 \times 10^{-6}$, thus showing that Eq. 9 expresses the best model for the experimental data. The interaction of the Met^{1606}-Arg^{1668} was characterized by a significant affinity, showing at pH 6.0 and 25°C a K_i value equal to ~1 μM, whereas α and β values were equal to 10 and 0.23, respectively, as shown in Fig. 5 *a*. These results are in agreement with a model where binding of the Met-containing peptide allosterically decreases by a factor ≈10 the affinity of the FRETS-VW73/ADAMTS13 interaction, and reduces ≈4-fold the k_{cat} value of the substrate cleavage. These effects are possible only if P2 in Scheme 2, binds to an exosite, distinct from the active site of the enzyme, whose ligation is able to affect the interaction with the substrate and the catalytic mechanism of the protease. The values of K_i, α, and β changed slightly but significantly as a function of pH in a range from 6.0 to 9.5 (Fig. 5, *b–d*). A trend to an increase of both K_i and β, and a decrease of α values was observed (Fig. 5, *b–d*). This result suggests that the interaction of P2 with ADAMTS13 involves the side chain of basic residues, and thus has a tendency to be weaker and to affect less efficiently the catalytic mechanisms at pH values >7.5. The use of shorter C-terminal VWF73 peptides, such as Met^{1606}-Phe^{1654}, Met^{1606}-Leu^{1657}, Met^{1606}-Ala^{1661}, and Met^{1606}-Leu^{1664}, variably inhibited the hydrolysis of FRETS-VWF73 (Fig. 6 *a*). In particular, a strong inhibition, approaching that one exerted by Met^{1606}-Arg^{1668}, was observed particularly when the peptides contained in their sequence Ala^{1661} and Leu^{1664} (Fig. 6 *b*).

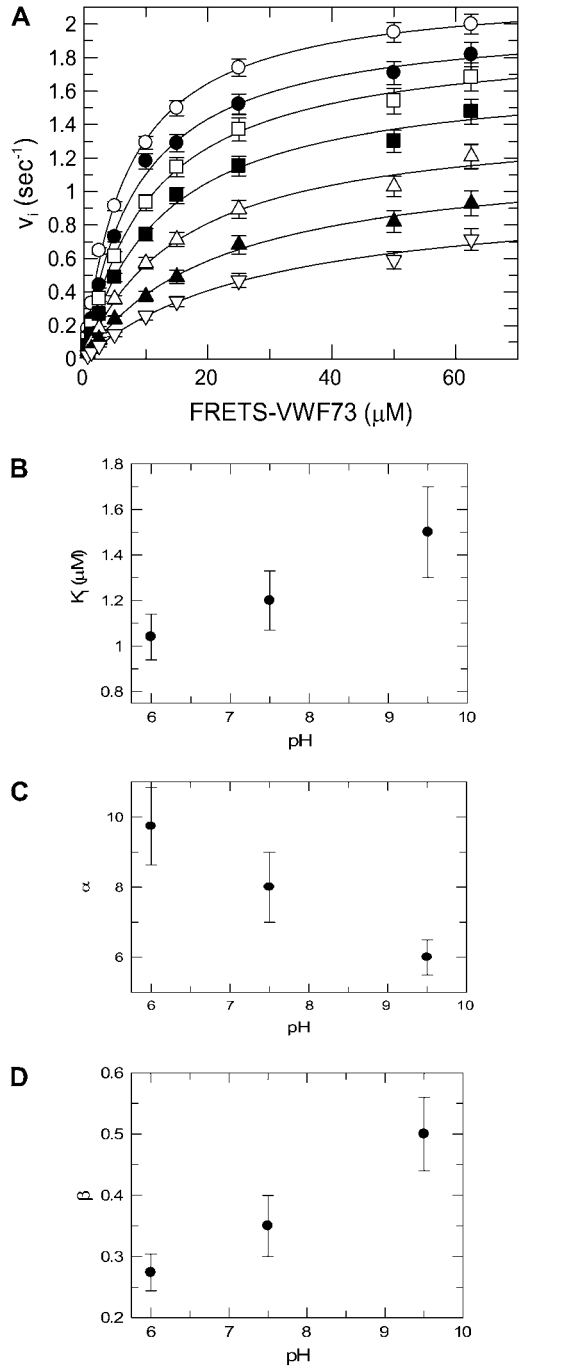

FIGURE 5 (*A*) Inhibition of ADAMTS13-catalyzed hydrolysis of FRETS-VWF73 by Met^{1606}-Arg^{1668} peptide used at the following concentrations: (O) zero, (●) 0.5 μM, (□) 1 μM, (■) 2 μM, (Δ) 4 μM, (▲) 8 μM, (∇) 16 μM. The experiment was carried out in four-buffer system (see text) at pH 7.50. Fifty-six experimental points were simultaneously fitted to a hyperbolic mixed-type inhibition equation (Eq. 9) with the best-fit parameter values $k_{cat} = 2.1 \pm 0.02$, $K_m = 6 \pm 0.2$ μM, $\alpha = 10 \pm 1$, $\beta = 0.23 \pm 0.02$. The vertical bars represent the SD from two different determinations. In the other panels the effect of pH on K_i (*B*), α (*C*), and β (*D*) parameter values of Eq. 9. are shown. The vertical bars represent the SD from two different determinations.

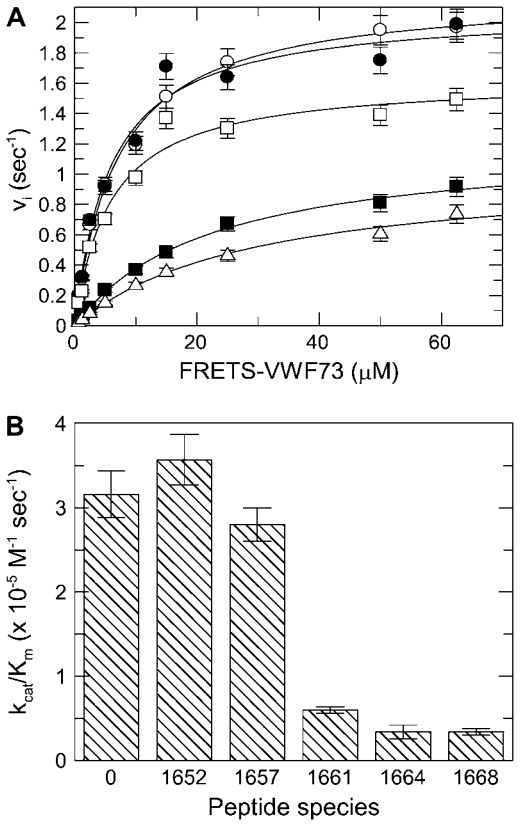

FIGURE 6 (*A*) Inhibition of ADAMTS13-catalyzed hydrolysis of FRETS-VWF73 by 20 μM of each of these VWF-derived peptides: Met^{1606}-Phe^{1654} (●), Met^{1606}-Leu^{1657} (□), Met^{1606}-Ala^{1661} (■), Met^{1606}-Leu^{1664} (Δ), and in absence of any peptide (O). The best fit k_{cat} and K_m values were 2.09 ± 0.09 sec^{-1} and 5.83 ± 0.9 μM, respectively, for Met^{1606}-Phe^{1654} (●), 1.63 ± 0.07 sec^{-1} and 5.83 ± 0.97 μM for Met^{1606}-Leu^{1657} (□), 1.21 ± 0.04 sec^{-1} and 22 ± 1.7 μM for Met^{1606}-Ala^{1661} (■), 1.04 ± 0.06 sec^{-1} and 30 ± 3.7 μM for Met^{1606}-Leu^{1664} (Δ). The best fit k_{cat} and K_m values were equal to 2.21 ± 0.05 sec^{-1} and 6.9 ± 0.06 μM in the absence of peptides (O). The vertical bars represent the SD from two different determinations. (*B*) Bar graph showing the measured k_{cat}/K_m values for hydrolysis of FRETS-VWF73 in the presence of 20 μM of the various C-terminal peptides of VWF73. The number reported for each peptide species refers to the number of the last amino acid in the peptide sequence, starting from Met^{1606}. The vertical bars represent the SD from two different determinations.

DISCUSSION

Some relevant findings emerged from this study: 1), two ionizable residues control the catalytic activity of ADAMTS13 toward FRETS-VWF73 over the pH range from 4.5 to 10.5; and 2), the pK_a of one group involved in the catalytic cycle can be reasonably assigned to the metal-bound water molecule, which generates the hydroxide species responsible for the cleavage of the substrate's peptide bond. Based on the findings in this study, the metal-bound water molecule is the natural candidate to act as a conduit for proton transfer (46). These results showed that the acidity of this ionizable group is dependent on the metal involved, and, from both theoretical and experimental standpoint, this behavior is typical of coordinated water molecules (41,43,47). The H_2O molecule bound to the ''harder'' Zn^{2+} ion, would render the metal-aquo complex a stronger Lewis acid than coordination to the ''softer'' Co^{2+} ion. About the almost complete inhibition of ADAMTS13 caused by Ni^{2+} insertion into the catalytic site, we hypothesize that this effect is consistent with a distorted tetrahedral coordination geometry of the metal ion, which is incompatible with an efficient alignment with the scissile bond.

Thus, the Zn^{2+} ion present in the catalytic site of ADAMTS13 and coordinated by His^{224}, His^{228}, and His^{234}, should be coordinated by the fourth ligand represented by a bound water molecule, which undergoes the metal-catalyzed dissociation:

$$Zn^{2+} + H_2O \rightarrow Zn^{2+}OH^- + H^+ \qquad (10)$$

The hydroxide species generated in the reaction acts as a nucleophile and attacks the peptide bond to be hydrolyzed (48). The findings that substitution of Zn^{2+} with Co^{2+} at the active site of ADAMTS13 causes a decrease of both the k_{cat} value and the pK_a value of the group involved in catalysis are in agreement with this mechanism. Ionization of His residues coordinating the zinc ion in the catalytic site could obviously contribute to the measured pK_{a1} value. The second ionizable group with a p$K_a \cong 4$ is likely represented by Glu^{225}, contained in the active site sequence from His^{224} to His^{234} bearing the residues coordinating the zinc ion. We could predict that a favorable hydrogen bond between this glutamate and the metal-bound water molecule would make the latter more nucleophilic. Compared to cobalt and nickel, zinc was the most efficient metal to ionize the catalytic water molecule responsible for the proteolytic activity of ADAMTS13. This effect likely depends also from the coordination geometry of metal ion and the position of the metal-bound water molecule. In fact, other metalloproteases, such as carboxypeptidase A and thermolysin, showed a higher catalytic specificity in the cleavage of their substrates upon the exchange of zinc with cobalt (41,49).

Although it is very likely that the acidic pK_a of the second catalytic residue could be assigned to Glu^{225}, as indicated in the Results section, we need to carefully interpret the experimental results. In fact, at pH <5 the protonation of the His imidazole side chain could affect the interaction with the zinc ion and consequently the catalytic cycle. These studies on the effect of temperature allowed us to have an estimate of the relevant kinetic rate constants and the relative activation energies of the catalytic steps of FRETS-VWF73 hydrolysis. In particular, from data listed in Table 1, it can be deduced that FRETS-VWF73 acts as a sticky substrate at pH 6.0 under temperatures <25°C, being the rate constant for the substrate dissociation from the active site comparable or even lower than that of its cleavage. This behavior renders the value of the k_{cat}/K_m similar to that of association rate constant of the substrate binding to the active site of ADAMTS13. By

contrast, at temperatures >25°C the dissociation rate is much higher than that of the cleavage rate, and the value of k_{cat}/K_m is about 10-fold lower than that of the association rate constant.

Furthermore, application of the Eyring's transition theory showed that the $\Delta S^{\ddagger}$ value is strongly negative. The activation entropy is a macroscopic quantity that includes a number of microscopic contributions by both the reactants and solvating molecules. Activation entropies are in many cases dominated by solvent reorganization effects (34). Activation entropy of catalytic interaction between VWF and ADAMTS13 is strongly negative, indicating that the transition state of this bimolecular interaction becomes more ordered by reducing considerable translational and rotational degrees of freedom of motion of the reactants. This result implies that the formation of the transition state requires the enzyme and the substrate to adopt discrete and precise conformations and solvent orientation. Thus, these findings indicate that ADAMTS13 recognizes and cleaves the Tyr-Met peptide bond in the A2 domain of VWF by lowering the activation entropy of the reaction due to positioning the two reactants and ordering metal-bound water in the active site. This mechanism is in accord with the extraordinary chemical and conformational specificity, which characterizes the catalytic interaction between VWF and ADAMTS13.

This mechanism is facilitated by the interactions of FRETS-VWF73 with exosites of the enzyme, that contribute to its correct and productive binding so that the catalytic water molecule is perfectly aligned toward the scissile bond of the substrate. Notably, the C-terminal product of ADAMTS13 hydrolysis, that is Met^{1606}-Arg^{1668} peptide, is able to bind with considerable affinity to ADAMTS13 and to inhibit it with a hyperbolic mixed-type mechanism. This result is in agreement with recent findings, showing that this VWF peptide binds to the spacer domain of ADAMTS13 (32,33). The experiments reported in this study show that the binding of FRETS-VWF73 to the enzyme reduces 6- to 10-fold the affinity of the Met^{1606}-Arg^{1668} peptide and vice-versa. The binding affinity of the Met^{1606}-Arg^{1668} peptide tends to decrease and have lower allosteric effects on both k_{cat} (resulting in higher β values) and K_m (resulting in lower α values) at pH >7.5, as shown in Fig. 5, *b–d*. No histidine residues are present in the Met^{1606}-containing peptide sequence, whereas in the spacer domain (Ser^{556}-Ala^{685} sequence) two histidine residues are present at position 1588 and 1594. Although the latter groups could be involved in the pH-dependence of the Met-containing peptide binding, a significant increase of the K_i of the Met-containing peptide occurs at pH > 8.5, where such groups should be already completely not protonated. This suggests the involvement in this interaction of ionizable residues with more basic pK_a values. Thus, the side chain of lysine or arginine residues may be engaged in this interaction. The molecular model of the FRETS-VWF73 and the prediction of the secondary folding of the spacer domain of ADAMTS13 provided some elements that could be useful to interpret these functional results from a structural point of view. These models showed that FRETS-VWF73 has an overall C-shaped scaffold ($\approx 40 \times \approx 40 \times \approx 25$ Å) with a helical C-terminal domain from D1653 to R1668 (Fig. 7). The FRETS-VWF73 molecule is mostly acidic (theoretical pI = 4.4), containing 6 basic and 11 acidic residues. Most of the charged residues are located after the Tyr^{1605}-Met^{1606} bond, such as the cluster composed of Asp^{1614} (VWF numbering system; Asp^{19} in the sequence of the peptide), Lys^{1617}, Arg^{1618}, Glu^{1638}, and Glu^{1640}, which cover a surface area of ~400 $Å^2$. Likewise, another mostly acidic cluster is composed of Asp^{1653}, Glu^{1655}, Glu^{1660}, Asp^{1663}, and the polar hydroxyl residue of Thr^{1656}. These residues, as mentioned previously, are contained in a helix located at the C terminus of the peptide and, as shown by the three-dimensional model, oppose the Tyr^{1605}-Met^{1606} peptide bond cleaved by ADAMTS13 at a mean distance of ~18/20 Å (Fig. 7, *inset*). The experimental findings shown in Fig. 6, *a* and *b*, showed that the product's region from Glu^{1660} and Arg^{1668} is necessary for an efficient inhibition of

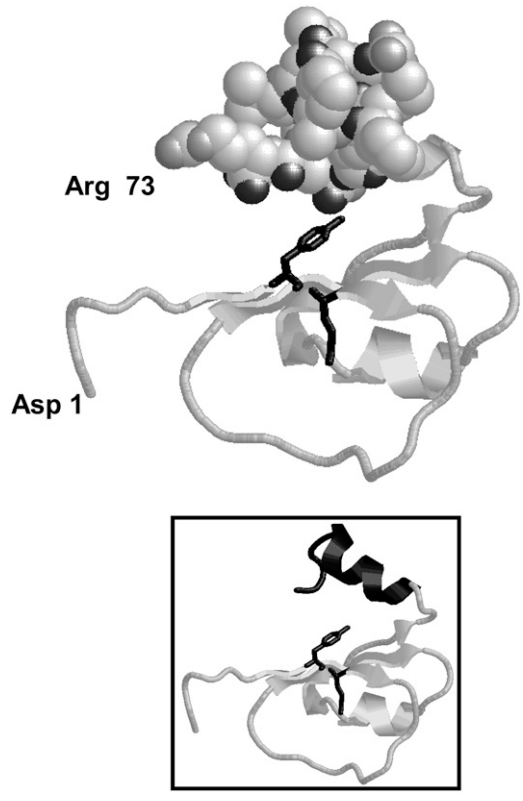

FIGURE 7 Three-dimensional molecular model of FRETS-VWF73. The residues 1 and 73 in FRETS -VWF73 refer to the primary sequence of the peptide substrate, whereas they correspond to residues Asp^{1596} and Arg^{1668} of VWF, respectively. The sequence from Thr^{1656} to Arg^{1668} in FRETS-VWF73 (VWF numbering system, Thr^{61} and Arg^{73}, respectively, in the primary sequence of FRETS-VWF73) are shown as filled space. In the FRETS-VWF73 model the side chain of both Tyr^{1605} and Met^{1606} are shown as black sticks. In the inset, the model of the peptide is shown as strands in the same orientation.

ADAMTS13, in agreement with recent studies (32). Thus, this helical region would bind to a part of the spacer domain using considerable ionic and polar interactions for the molecular recognition. Without known three-dimensional structures homologous to the spacer domain of ADAMTS13, just a secondary structure prediction of this region can be given in consideration of the lack of cysteine residues, and thus of constraints dictated by the disulfide-bonding connectivity. The ADAMTS13 spacer domain is positively charged (theoretical pI = 9.51), containing 15 (11.5%) Arg and three (2.3%) Lys residues. The secondary structure prediction carried out by the PsiPred program showed that this domain should be mostly composed of strands (see Fig. S3 in Data S1) with more disordered regions only at the ends of N- and C-terminal regions. As a consequence, this domain should assume mainly a stretched configuration. This finding is in agreement with the ''connecting'' nature of this domain, which links the metalloprotease/disintegrin/Cys-rich domain with the TSP-1 repeats of the enzyme (5). Moreover, this domain should be extensively exposed to solvent, as it represents often the main target for auto-antibodies produced in immunomediated thrombotic microangiopathies (50). At its maximal theoretical extension the spacer domain is 195 Å long, so we can predict from simple geometrical considerations that only the N-terminal region extending from Ser^{1556} to Ala^{1586} and containing three Arg and one Lys residues could interact with the acidic C-terminal region of FRETS-VWF73. Based on these biochemical and modeling results, it is likely that the enzyme has a C-shaped scaffold, so that the spacer domain should oppose the active site of the metalloprotease to accommodate the entire FRETS-VWF73 molecule that, according to the model reported in Fig. 7, has a similar and complementary C-shaped conformation. Due to dimensions of the various enzyme domains and the conformation of the VWF73 substrate, only this particular tertiary structure of ADAMTS13 could allow an efficient interaction with FRETS-VWF73. Notably, the C-shaped scaffold was also observed in the recently solved structure of ADAMTS-1, where the Cys-rich domain, flanking the spacer region of the metalloprotease in the ADAMTS family, stacks against the active site of the enzyme (51). The charged residues of both VWF and ADAMTS13 could serve to preorient correctly the enzyme and the substrate. The interaction with the spacer domain would favor the molecular recognition of VWF. This conclusion was also supported by the finding that a shorter FRETS-VWF substrate (from Asp^{1596} to Phe^{1654}) was minimally recognized and hydrolyzed by ADAMTS13, at pH 6.00 and 37°C (data not shown). The involvement of this exosite favors a correct and efficient orientation of the VWF molecule toward the catalytic pocket of ADAMTS13, where the zinc-bound water molecule can properly face the scissile Tyr-Met bond, carrying out the catalytic cleavage. Moreover, once sufficient concentrations of C-terminal product is formed, binding of the C-terminal cleaved product to the spacer domain induces an inhibitory allosteric control of the ADAMTS13 activity, likely aimed at limiting an excessive loss of high molecular weight multimers of VWF. The relevance of the VWF Met^{1606}-Arg^{1668} sequence for the molecular recognition by the protease is also shown by the strong inhibitory effect exerted by auto-antibodies, which interact with the spacer domain of ADAMTS13, often present in thrombotic microangiopathies (50).

Notably, a recent study with recombinant VWF constructs carrying mutations responsible for the occurrence of a type 2A Von Willebrand disease showed that these VWF molecules are characterized by an exalted hydrolysis by ADAMTS13 (7). Among these VWF molecules, the authors indicated several mutations located in the region from Met^{1606} to Arg^{1668} such as Val^{1607}Asp, Gly^{1609}Arg, Ile^{1628}Thr, Gly^{1629}Glu, Gly^{1631}Asp, and Glu^{1638}Lys (7). Based on the results of this study, we can hypothesize that these mutations, and especially the charge reversal at position 1638 of VWF, affect the interaction of VWF with the spacer domain of ADAMTS13, thus perturbing the negative feed back mechanism of VWF cleavage described above and favoring its degradation

In conclusion, the study of the pH- and temperature-dependence of the ADAMTS13 activity provided novel findings to address the knowledge of the intermediate steps of the catalytic cycle of the metalloprotease. Furthermore, the Met-containing peptide produced by cleavage at the Tyr^{1605}-Met^{1606} peptide bond is able to allosterically inhibit the enzyme's function. In this study, we showed that pH-dependent interactions between acidic residues from Met^{1606} and Arg^{1668} of VWF A2 domain and basic residues of the spacer domain of ADAMTS13 play a central role in this allosteric mechanism. Further studies are needed to assess whether the binding of particular auto-antibodies to the spacer domain of ADAMTS13, responsible for acquired forms of thrombotic microangiopathies, could directly trigger this allosteric mechanism, inhibiting the interaction with VWF multimers.

SUPPLEMENTARY MATERIAL

To view all of the supplemental files associated with this article, visit www.biophysj.org.

R.D.C. is grateful to Dr. S. Rutella (Catholic University School of Medicine, Rome) for critical reading of the manuscript and providing useful suggestions. The Protein Data Bank files of the molecular models of FRETS-VWF73 are available on request at: rdecristofaro@rm.unicatt.it.

This study was supported by the Italian Ministry of University and Research (''ex-60%'', 2006, and ''PRIN 2005'').

REFERENCES

1. Chung, D. W., and K. Fujikawa. 2002. Processing of von Willebrand factor by ADAMTS-13. *Biochemistry*. 41:11065–11070.
2. Dent, J. A., S. D. Berkowitz, J. Ware, C. K. Kasper, and Z. M. Ruggeri. 1990. Identification of a cleavage site directing the immunochemical

detection of molecular abnormalities in type IIA von Willebrand factor. *Proc. Natl. Acad. Sci. USA.* 87:6306–6310.

3. Tsai, H. M. 1996. Physiologic cleavage of von Willebrand factor by a plasma protease is dependent on its conformation and requires calcium ion. *Blood.* 87:4235–4244.
4. Fischer, B. E., K. B. Thomas, U. Schlokat, and F. Dorner. 1998. Triplet structure of human von Willebrand factor. *Biochem. J.* 331:483–488.
5. Koo, B. H., D. Oh, S. Y. Chung, N. K. Kim, S. Park, Y. Jang, and K. H. Chung. 2002. Deficiency of von Willebrand factor-cleaving protease activity in the plasma of malignant patients. *Thromb. Res.* 105:471–476.
6. Rayes, J., A. Hommais, P. Legendre, H. Tout, A. Veyradier, B. Obert, A. S. Ribba, and J. P. Girma. 2007. Effect of von Willebrand disease type 2B and type 2M mutations on the susceptibility of von Willebrand factor to ADAMTS-13. *J. Thromb. Haemost.* 5:321–328.
7. Hassenpflug, W. A., U. Budde, T. Obser, D. Angerhaus, E. Drewke, S. Schneppenheim, and R. Schneppenheim. 2006. Impact of mutations in the von Willebrand factor A2 domain on ADAMTS13-dependent proteolysis. *Blood.* 107:2339–2345.
8. Furlan, M., R. Robles, and B. Lamie. 1996. Partial purification and characterization of a protease from human plasma cleaving von Willebrand factor to fragments produced by in vivo proteolysis. *Blood.* 87:4223–4234.
9. Levy, G. G., W. C. Nichols, E. C. Lian, T. Foroud, J. N. McClintick, B. M. McGee, A. Y. Yang, D. R. Siemieniak, K. R. Stark, R. Gruppo, R. Sarode, S. B. Shurin, V. Chandrasekaran, S. P. Stabler, H. Sabio, E. E. Bouhassira, J. D. Upshaw, Jr., D. Ginsburg, and H. M. Tsai. 2001. Mutations in a member of the ADAMTS gene family cause thrombotic thrombocytopenic purpura. *Nature.* 413:488–494.
10. Moake, J. L. 2002. Thrombotic microangiopathies. *N. Engl. J. Med.* 347:589–600.
11. Tsai, H. M., I. I. Sussman, D. Ginsburg, H. Lankhof, J. J. Sixma, and R. L. Nagel. 1997. Proteolytic cleavage of recombinant type 2A von Willebrand factor mutants R834W and R834Q: inhibition by doxycycline and by monoclonal antibody VP-1. *Blood.* 89:1954–1962.
12. O'Brien, L. A., J. J. Sutherland, D. F. Weaver, and D. Lillicrap. 2005. Theoretical structural explanation for Group I and Group II, type 2A von Willebrand disease mutations. *J. Thromb. Haemost.* 3:796–797.
13. Dong, J. F. 2005. Cleavage of ultra-large von Willebrand factor by ADAMTS-13 under flow conditions. *J. Thromb. Haemost.* 3:1710–1716.
14. Sutherland, J. J., L. A. O'Brien, D. Lillicrap, and D. F. Weaver. 2004. Molecular modeling of the von Willebrand factor A2 Domain and the effects of associated type 2A von Willebrand disease mutations. *J. Mol. Model.* 10:259–270.
15. O'Brien, L. A., P. D. James, M. Othman, E. Berber, C. Cameron, C. R. Notley, C. A. Hegadorn, J. J. Sutherland, C. Hough, G. E. Rivard, D. O'Shaunessey, and D. Lillicrap. 2003. Founder von Willebrand factor haplotype associated with type 1 von Willebrand disease. *Blood.* 102:549–557.
16. Dong, J. F., J. L. Moake, L. Nolasco, A. Bernardo, W. Arceneaux, C. N. Shrimpton, A. J. Schade, L. V. McIntire, K. Fujikawa, and J. A. Lopez. 2002. ADAMTS-13 rapidly cleaves newly secreted ultralarge von Willebrand factor multimers on the endothelial surface under flowing conditions. *Blood.* 100:4033–4039.
17. Tsai, H. M., I. I. Sussman, and R. L. Nagel. 1994. Shear stress enhances the proteolysis of von Willebrand factor in normal plasma. *Blood.* 83:2171–2179.
18. Nishio, K., P. J. Anderson, X. L. Zheng, and J. E. Sadler. 2004. Binding of platelet glycoprotein Ibα to von Willebrand factor domain A1 stimulates the cleavage of the adjacent domain A2 by ADAMTS13. *Proc. Natl. Acad. Sci. USA.* 101:10578–10583.
19. Shim, K., P. J. Anderson, E. A. Tuley, E. Wiswall, and J. E. Sadler. 2008. Platelet-VWF complexes are preferred substrates of ADAMTS13 under fluid shear stress. *Blood.* 111:651–657.
20. De Cristofaro, R., F. Peyvandi, R. Palla, S. Lavoretano, R. Lombardi, G. Merati, F. Romitelli, E. Di Stasio, and P. M. Mannucci. 2005. Role of chloride ions in modulation of the interaction between von Willebrand factor and ADAMTS-13. *J. Biol. Chem.* 280:23295–23302.
21. De Cristofaro, R., F. Peyvandi, L. Baronciani, R. Palla, S. Lavoretano, R. Lombardi, E. Di Stasio, A. B. Federici, and P. M. Mannucci. 2006. Molecular mapping of the chloride-binding site in von Willebrand factor (VWF): energetics and conformational effects on the VWF/ADAMTS-13 interaction. *J. Biol. Chem.* 281:30400–30411.
22. Kokame, K., Y. Nobe, Y. Kokubo, A. Okayama, and T. Miyata. 2005. FRETS-VWF73, a first fluorogenic substrate for ADAMTS13 assay. *Br. J. Haematol.* 129:93–100.
23. Fasciglione, G. F., S. Marini, S. D'Alessio, V. Politi, and M. Coletta. 2000. pH- and temperature-dependence of functional modulation in metalloproteinases. A comparison between neutrophil collagenase and gelatinases A and B. *Biophys. J.* 79:2138–2149.
24. Cha, J., M. V. Pedersen, and D. S. Auld. 1996. Metal and pH dependence of heptapeptide catalysis by human matrilysin. *Biochemistry.* 35:15831–15838.
25. Plaimauer, B., K. Zimmermann, D. Volkel, G. Antoine, R. Kerschbaumer, P. Jenab, M. Furlan, H. Gerritsen, B. Lammle, H. P. Schwarz, and F. Scheiflinger. 2002. Cloning, expression, and functional characterization of the von Willebrand factor-cleaving protease (ADAMTS13). *Blood.* 100:3626–3632.
26. Pace, C. N., F. Vajdos, L. Fee, G. Grimsley, and T. Gray. 1995. How to measure and predict the molar absorption coefficient of a protein. *Protein Sci.* 4:2411–2423.
27. Fersht, A. 1985. Enzyme Structure and Mechanism. Freeman, New York.
28. Ayala, Y. M., and E. Di Cera. 2000. A simple method for the determination of individual rate constants for substrate hydrolysis by serine proteases. *Protein Sci.* 9:1589–1593.
29. Laidler, K. 1965. Chemical Kinetics. McGraw-Hill, New York.
30. Di Stasio, E., P. Bizzarri, F. Misiti, E. Pavoni, and A. Brancaccio. 2004. A fast and accurate procedure to collect and analyze unfolding fluorescence signal: the case of dystroglycan domains. *Biophys. Chem.* 107:197–211.
31. Di Cera, E., R. De Cristofaro, D. J. Albright, and J. W. Fenton 2nd. 1991. Linkage between proton binding and amidase activity in human alpha-thrombin: effect of ions and temperature. *Biochemistry.* 30:7913–7924.
32. Gao, W., P. J. Anderson, E. M. Majerus, E. A. Tuley, and J. E. Sadler. 2006. Exosite interactions contribute to tension-induced cleavage of von Willebrand factor by the antithrombotic ADAMTS13 metalloprotease. *Proc. Natl. Acad. Sci. USA.* 103:19099–19104.
33. Wu, J. J., K. Fujikawa, B. A. McMullen, and D. W. Chung. 2006. Characterization of a core binding site for ADAMTS-13 in the A2 domain of von Willebrand factor. *Proc. Natl. Acad. Sci. USA.* 103:18470–18474.
34. Segel, I. H. 1975. Enzyme Kinetics: Behavior and Analysis of Rapid Equilibrium and Steady State Enzyme Systems. Wiley, New York.
35. Reference deleted in proof.
36. Jones, D. T. 1999. Protein secondary structure prediction based on position-specific scoring matrices. *J. Mol. Biol.* 292:195–202.
37. McGuffin, L. J., K. Bryson, and D. T. Jones. 2000. The PSIPRED protein structure prediction server. *Bioinformatics.* 16:404–405.
38. Snider, C. E., J. C. Moore, T. E. Warkentin, C. N. Finch, C. P. Hayward, and J. G. Kelton. 2004. Dissociation between the level of von Willebrand factor-cleaving protease activity and disease in a patient with congenital thrombotic thrombocytopenic purpura. *Am. J. Hematol.* 77:387–390.
39. Zanardelli, S., J. T. Crawley, C. K. Chion, J. K. Lam, R. J. Preston, and D. A. Lane. 2006. ADAMTS13 substrate recognition of von Willebrand factor A2 domain. *J. Biol. Chem.* 281:1555–1563.
40. Tipton, K. F., and H. B. Dixon. 1979. Effects of pH on enzymes. *Methods Enzymol.* 63:183–234.
41. Auld, D. S., and B. L. Vallee. 1970. Kinetics of carboxypeptidase A. The pH dependence of tripeptide hydrolysis catalyzed by zinc, cobalt, and manganese enzymes. *Biochemistry.* 9:4352–4359.
42. Huang, D. T., M. A. Thomas, and R. I. Christopherson. 1999. Divalent metal derivatives of the hamster dihydroorotase domain. *Biochemistry.* 38:9964–9970.

43. Cross, J. B., J. S. Duca, J. J. Kaminski, and V. S. Madison. 2002. The active site of a zinc-dependent metalloproteinase influences the computed pK(a) of ligands coordinated to the catalytic zinc ion. *J. Am. Chem. Soc.* 124:11004–11007.

44. Kitzinger, C., and R. Hems. 1959. Enthalpies of hydrolysis of glutamine and asparagine and of ionization of glutamic and aspartic acids. *Biochem. J.* 71:395–400.

45. Cornish-Bowden, A. 1995. Fundamentals of enzyme kinetics. Portland Press, London.

46. Kluger, R., A. K. Dodds, and M. K. Wong. 1984. Variation of steric effects in metal ion catalyzed proton transfer. a probe of transition-state structure. *J. Am. Chem. Soc.* 106:1113–1117.

47. Makinen, M. W., L. C. Kuo, J. J. Dymowski, and S. Jaffer. 1979. Catalytic role of the metal ion of carboxypeptidase A in ester hydrolysis. *J. Biol. Chem.* 254:356–366.

48. Auld, D. S. 2004. Catalytic Mechanisms for Metallopeptidases. Elsevier Academic Press, New York.

49. Holmquist, B., and B. L. Vallee. 1974. Metal substitutions and inhibition of thermolysin: spectra of the cobalt enzyme. *J. Biol. Chem.* 249:4601–4607.

50. Klaus, C., B. Plaimauer, J. D. Studt, F. Dorner, B. Lammle, P. M. Mannucci, and F. Scheiflinger. 2004. Epitope mapping of ADAMTS13 autoantibodies in acquired thrombotic thrombocytopenic purpura. *Blood.* 103:4514–4519.

51. Gerhardt, S., G. Hassall, P. Hawtin, E. McCall, L. Flavell, C. Minshull, D. Hargreaves, A. Ting, R. A. Pauptit, A. E. Parker, and W. M. Abbott. 2007. Crystal structures of human ADAMTS-1 show a conserved catalytic domain and a disintegrin-like domain with a fold homologous to cysteine-rich domains. *J. Mol. Biol.* 373: 891–902.